(NASA-CR-189313) UV SPECTRAL
VARIABILITY IN THE HERBIG Ae STAR
HR 5999. 11: THE ACCRETION
INTERPRETATION (Computer Sciences
Corp.) 11 p

N94-23334

Unclas

G3/89   0198347

UV spectral variability in the Herbig Ae star HR 5999

XI. The accretion interpretation[*]

M.R. Pérez[1], C.A. Grady[2], and P.S. Thé[3]

[1] Astronomy Programs-CSC, IUE Observatory-Code 684.9, NASA-GSFC, Greenbelt, MD 20771, USA
[2] Applied Research Corp., Suite 1120, 8201 Corporate Dr., Landover, MD 20785, USA
[3] Astronomical Institute "Anton Pannekoek", University of Amsterdam, Kruislaan 403, NL-1098 SJ Amsterdam, The Netherlands

Abstract. We report recent IUE high- and low-dispersion observations with the IUE long wavelength camera (LWP) and short wavelength camera (SWP) of the Herbig Ae star HR 5999. We have found a dramatic change in the structure of the Mg II h and k lines (2795.5, 2802.7 Å) along with some continuum flux excesses especially at the short end of the SWP camera. LWP high-dispersion observations of HR 5999 obtained between 1979 and 1990, at times of comparatively low UV continuum fluxes, exhibit P Cygni type III profiles in the Mg II resonance doublet. In contrast, observations made from September 1990 through March 16-18, 1992, with high UV continuum fluxes, present Mg II lines with reverse P Cygni profiles indicative of some active episodic accretion. Accreting gas can also be detected in the additional red wings of the various Fe II and Mn II absorption lines, with velocities up to +300-350 km s^{-1} (September 1990). By September 10, 1992 the Mg II profile had returned to the type III P Cygni profile similar to those from earlier spectra. The correlation between the presence of large column densities of accreting gas and the continuum light variations supports suggestions by several authors that HR 5999 is surrounded by an optically thick, viscously heated accretion disk. Detection of accreting gas in the line of sight to HR 5999 permits us to place constraints on our viewing geometry for this system. A discussion is included comparing the spectral and physical similarities between HR 5999 and the more evolved proto-planetary candidate system, β Pictoris.

Key words: stars: pre-main sequence – stars: variable – accretion: accretion disks – stars: individual: HR 5999 – accretion – HR 5999

1. Introduction

The irregular variable star HR 5999 (HD 144668, V856 Sco, CPD -38° 6373) has been intensively monitored in the last decade at almost every wavelength available to observational astronomers. In particular, this star has shown quasi-periodic and random photometric and spectroscopic variabilities recently summarized by Tjin A Djie et al. (1989), Praderie et al. (1991) and Pérez et al. (1992a). Three recent studies have suggested that many of the features of the circumstellar environment of HR 5999 can be accounted for by the presence of an optically thick accretion disk. Blondel et al. (1993) suggested the presence of such a disk as a result of their analysis of the extended Lyα emission around HR 5999. Pérez et al. (1992a) have suggested instabilities in an accretion disk as the source of non-periodic photometric variability in the optical. More recently, Hillenbrand et al. (1992) have interpreted the infrared excess of HR 5999 in terms of a large, optically thick debris disk with a high accretion rate and possible inner cavity.

In an underplayed observational feature of Hα, Baade & Stahl (1989) barely mentioned that the Hα lines of HR 5999 appeared to be like inverse Beals (1950) type III P Cygni profiles during the nights of June 7 and 8 in 1987. This immediately suggested that we might be able to sample accreting gas in the line of sight to HR 5999. Since it has been known that Mg II lines (2800 Å) are being formed in more extended regions than Hα (up to 50 stellar radii) we started monitoring HR 5999 in the LWP high-dispersion mode on September 7, 1990. Our first observation confirmed the prediction that Mg II lines in HR 5999 are a good tracer of the dynamics in extended shells and/or bipolar flows by appearing as an inverse type III P Cygni profile, similar to Hα, indicating the increase of accretion phenomena in the line of sight.

In this paper, we present IUE high and low dispersion spectroscopic observations obtained during the last 3 years, together with an overview of the earlier spectra. We find UV continuum light variations are particularly noticeable longward of 1530 Å, and are correlated with the presence of elevated column densi-

A+A	Autor M.R. Pérez	Proof-Seiten 10
Makroscript-Nr.	MS-Seiten 10	Versand-Datum 16. 11. 1992

2. Observations

Between 1978 and late-1992, HR 5999 has been observed 51 times in high- and low-dispersion with both the long- (LW) and short-wavelength (SW) cameras. Some of the relevant results from the high-dispersion data have been reported by Blondel et al. (1989). In the LW high-dispersion mode this star has been monitored in thirteen occasions since 1979, including the 5 observations made since September 1990 under our IUE observing programs. A journal of the observations considered in this study is listed in Table 1.

3. Data reduction

3.1. Low dispersion data

The IUE low dispersion spectra were processed using the version of the IUE Spectral Image Processing System (IUESIPS) in use at the time of archiving (see Turnrose and Thompson 1984). The earliest 7 spectra of HR 5999 (LWR 1442, 1465, 1511, 1558 and SWP 1486, 1514, and 1569) were obtained during the IUE commissioning period. Subsequent calibration analysis has demonstrated that the IUE cameras were undergoing considerable sensitivity and flat-field changes during this period, which were not adequately monitored by the rather sparse calibration observations. As a result, we have excluded these data from subsequent analysis. The absolute calibration data for the LWR and SWP data are from Bohlin and Holm (1980), and the LWP is from Cassatella and Harris (1983). No compensation for the slow loss of camera sensitivity with time has been made for the SWP and LWP data since the effect is small (Teays and Garhart 1990). The LWR sensitivity degradation correction is due to Clavel, Gilmozzi, and Prieto (1985).

3.2. Estimated V magnitudes using the IUE Fine Error Sensor

The IUE Fine Error Sensor (FES) routinely obtains broadband visual photometry in conjunction with the UV spectra. We have calculated the equivalent V-band magnitudes using the calibration of Pérez and Loomis (1991) (Table 1), which compensates for the sensitivity loss of the FES, the use of difference reference points within the FES over the course of the IUE mission, and the telescope focus. We have used an average value of (B–V)=0.31 to correct for color effects. The uncertainty in the V(FES) magnitudes is estimated to be $\pm 0^m.05$.

3.3. High dispersion data

All of the LW high dispersion data have been processed using the IUE Spectral Image Processing System (IUESIPS) described in Turnrose and Thompson (1984), which accounts for thermally-induced shifts in the spectral format. The subsequent reduction used the Ake (1982) and the Ake (1985) echelle blaze function data for the LWR and LWP respectively. The absolute calibration data for the high dispersion spectra are taken from Cassatella et al. (1989) with no compensation for the slow loss of sensitivity of the cameras with time. Following calibration, reseaux-contaminated and saturated portions of the spectrum have been replaced using estimates based on a

linear interpolation of the flux levels from adjacent good data points. The spectra have also been smoothed by a 5-point mean filter, resulting in a typical signal-to-noise near 2800 Å of 10–12. Small offsets in the radial velocity scale, of order 5 km s^{-1} or less are consistent with the 1″ pointing accuracy of the IUE (Harris and Sonneborn, 1987). As noted in Boggess et al. (1991), the LWP spectra exhibit an approximately +10 km s^{-1} offset relative to the HST GHRS calibration which is in good agreement with heliocentric velocity scales. No compensation for this effect has been made in our data.

4. UV photometric variation and the spectral energy distributions

4.1. The UV continuum variability

A striking feature of HR 5999 in the optical is the pronounced photometric variability. As shown in Figure 1, the continuum exhibits significant variability down to at least 1450 Å. In the longer wavelength portion of the spectrum near the Mg II resonance doublet, the continuum luminosity can be grouped into a UV-bright state and a UV-faint state, with up to a magnitude difference in flux levels between the states. The UV bright state at 2815 Å has been observed only for V(FES)<7.0. At 1630 Å, faint and bright states are observed, but the association with V(FES) is less apparent. UV-bright states are observed down to V(FES)=7.46, while fainter spectra are observed over the same range as at 2815 Å. The 1450 Å data exhibit significant variation which does not appear correlated with the continuum flux at longer wavelengths. In all spectra, even those obtained in the UV-faintest states observed to date, the IUE spectra provide convincing evidence for a continuum UV excess compared to similarly exposed A5-A7 standard star spectra down to Lyα.

4.2. Correction for interstellar and circumstellar extinction

It has been known for some time that the extinction law towards HR 5999 is quite anomalous (Thé and Tjin A Djie 1978, Paper I, Thé et al. 1981, Paper V, Hecht et al. 1984), typical of other active star-forming regions, such as Orion. Preliminary estimates of the ratio of total to selective extinction, $R_v = \frac{A_v}{E(B-V)}$, accounting for both the foreground and circumstellar extinctions, were between 4 and 5. Our trial-and-error fit of the unreddened optical fluxes to the Kurucz models indicated an R_v value of ~ 5.5–5.7. The latest R_v value based on Strömgren photometric data derived from 282 data points covering 7 years of monitoring, is 5.8 (Pérez et al. 1992a). This value is intended to be an average since R_v becomes smaller when the star gets brighter as acknowledged by Thé et al. (1985) and Pérez et al. (1992a). By using this value of R_v and equation (1) in Pérez et al. (1992a) we have determined the value of (B–V), for a given V(FES) as explained in §3.2. We have selected a pair of well-exposed SW and LW images from Table 1 representative of the low and high states. The low-dispersion images SWP 21276 and LWR 16970 represent the UV spectral response when the V(FES) indicated a value of 7.3. Similarly, the images SWP 26369 and LWP 6364 are representative of a high state; the mean V(FES) is 6.8. The color excesses, E(B–V), were then derived using the calibration of Schmidt-Kaler (1982) of (B–V)$_o$=+0.22 for a A7 III spectral type. We have also assumed that in the UV-faint state the

underlying proto-star is more easily detected, yielding a more realistic correction for the color excess, E(B-V). Subsequently, the unreddened UV fluxes using E(B-V) obtained from the UV-faint state, were derived by using the parametrization of the R_v value for 5.8 described by Cardelli, Clayton and Mathis (1989).

Since lines of sight with large values of R_v are known to produce small UV extinction in the near and far-UV, the extinction correction is rather insensitive for values of $5.5 \leq R_v \leq 5.8$, feature which strengthen the conclusions obtained in this treatment. The unreddened UV fluxes shown in Figure 2 present the comparison with three Kurucz (1991) models covering the range of A5-A8 III (Schmidt-Kaler 1982), with T_{eff}=8000, 7750, and 7500, log g=3.5, log z=0 scaled at λ=5550 Å according to the V(FES) magnitudes. We note that even in the UV-faint state (Figure 2; upper panel), the continuum flux mimics a A5 III at these wavelengths with detectable excess shortward of 1600 Å and longward of 2600 Å. The fact that the absorption features appear stronger in the UV-bright state suggest that we are not looking directly into the hot boundary layer or inner accretion disk, but through an optically thick shell, nearly edge-on, which mimics a photosphere. From the high-dispersion data we have observed that the additional pseudo absorption lines, seen in the high state, are primarily associated with the changes in Fe opacity (e.g., Fe II).

A trend of inferred spectral type shifting to earlier types with decreasing wavelength, larger UV excesses during episodes of high optical luminosity, and a flux distribution which is not consistent with a single-temperature stellar model, has previously been observed in lower mass pre-main sequence (PMS) stars, particularly in stars undergoing FU Orionis-type (FUOR) outbursts (Hartmann and Kenyon 1985). These phenomena have been interpreted as evidence for the presence of emission from an optically thick accretion disk and boundary layer. Our data provide the first detection of similar phenomena in a more massive protostar. The extent of the UV excess, even in the faintest UV spectra obtained to date is such that we would not expect to detect the stellar photosphere.

4.3. The emission lines

The spectrum of HR 5999 shortward of 1600 Å is rich in emission lines from species commonly associated with chromospheres in late-type stars. The only emission lines which can be confidently identified in all of the program spectra, which cover a wide range in signal-to-noise at these wavelengths, are the 2 strongest, O I 1302 Å and C IV 1549Å. Lyα emission from HR 5999 in the 2 high dispersion SWP spectra has been studied by Blondel et al. (1992). The circumstellar Lyα emission is blended with geocoronal emission at the resolution of the IUE low dispersion data considered here, and thus will not be further discussed. Both O I and C IV exhibit significant variation in net emission fluxes and in the velocity range covered by the emission. The net fluxes and velocity widths are smaller in the UV-faint spectra compared to the UV-bright spectra (Figure 3). The UV-faint spectra show much less scatter than is observed in the UV-bright data. A distinctive feature of the C IV emission is the variability in the emission centroid. In general, the C IV emission characteristics show more scatter than O I, suggesting at least partial formation in a somewhat different region. Blondel et al. (1992) reached similar conclusions in a comparison of O I and Lyα in high dispersion IUE SW spectra.
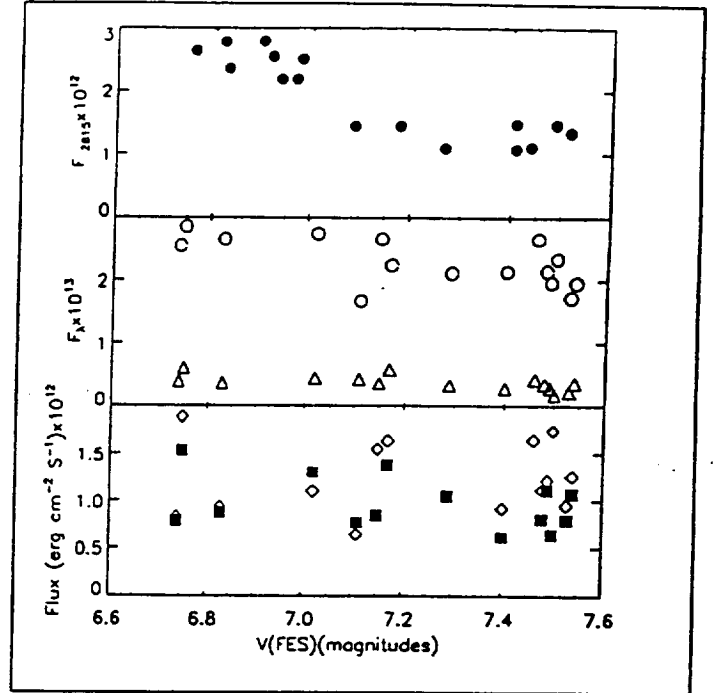

Fig. 1. UV photometric variability in HR 5999 of the observed fluxes as a function of the derived visual magnitude V(FES). Continuum variability at 2815 Å (filled circles), 1620 Å (open circles), 1450 Å (triangles) is shown. Net observed emission fluxes for C IV (filled squares) and O I (diamonds) are also indicated.

5. The line profiles

The UV spectrum of HR 5999 is rich in lines originating in the circumstellar envelope which can be used to test our conclusions, based on the low dispersion data, that the UV spectrum should be dominated by features originating in an accretion disk or boundary layer. For the purposes of our study we will consider the Mg II resonance doublet, which exhibits both emission and a central reversal to saturated absorption, and lines from singly ionized iron-peak elements which exhibit only absorption profiles.

5.1. Mg II emission

An observational study of the shape of the Mg II lines in bright Herbig Ae/Be (HAEBE) stars by Pérez, Imhoff and Thé (1992b) has shown that there is a smooth progression of profiles ranging from well-developed type III P Cyg for the youngest to narrow absorption lines for the stars with more main sequence characteristics. For the truly PMS among the HAEBE sample, the Mg II profiles are unique when compared with B main sequence and Be classical stars and are generally the signature of accelerating winds in their extended circumstellar disks (between 315 and 495 km s^{-1} in the case of the extreme object AB Aur, Praderie et al. 1986).

The Mg II profiles in HR 5999 are similar in shape when compared with the youngest members in the HAEBE class, but they are also substantially narrower. It is believed that this is due to the viewing stellar geometry, nearly edge-on, and due to the fact that a part of the Mg II lines are probably

Table 1. IUE Journal of Observations from 1979-1992. Where multiple, graded exposures were obtained on the same date, continuum measurements are tabulated for the spectrum with the best exposure in the wavelength of interest. Exposure times for the spectra are given in minutes (large/small aperture). The continuum flux units are erg cm^{-2} s^{-1} Å^{-1} and the line fluxes are given in erg cm^{-2} s^{-1}. The uncertainties for the emission line fluxes range between 5% for the best exposed data to 20% for the less well exposed spectra.

| Year	Date	Image	T_{esp}	Disp.	V(FES)	$F_{2815} \times 10^{12}$	$F_{1620} \times 10^{12}$	$F_{1450} \times 10^{13}$	C IV	O I
1979	11 Mar	LWR 3980	50	Hi	6.92	2.54±.24				
	19 Mar	LWR 4067	118	Hi	6.82	2.78±.31				
1980	31 Aug	SWP 9973	12	Low	6.75		.29±.01	.61±.06	1.53	1.89
	31 Aug	SWP 9974	355	Hi	6.74					
1982	26 Aug	LWR 14016	100	Hi	7.49	1.45±.15				
	26 Aug	SWP 17780	30	Low	7.48		.22±.01	.35±.05	0.81	1.12
	27 Aug	SWP 17789	30	Low	7.54		.20±.02	.37±.04	1.07	1.26
	27 Aug	LWR 14026	100	Hi	7.52	1.33±.11				
	28 Aug	SWP 17790	12	Low	7.53		.17±.016	.23±.08	0.80	0.95
	28 Aug	LWR 14027	8	Low	7.55					
1983	02 Jun	LWR 16060	30	Low	7.41	1.46±.09				
	02 Jun	SWP 20133	18	Low	7.40		.21±.03	.29±.11	0.62	0.92
	31 Aug	LWR 16706	3	Low	7.15					
	31 Aug	LWR 16707	12	Low	7.18	1.43±.08				
	31 Aug	SWP 20861	6	Low	7.16					
	31 Aug	SWP 20862	10	Low	7.16					
	31 Aug	SWP 20863	40	Low	7.17		.23±.03	.18±.26	0.64	1.75
	11 Sep	LWR 16768	8/3	Low	7.09					
	11 Sep	LWR 16769	110	Hi	7.09	1.43±.14				
	11 Sep	SWP 21020	26/5	Low	7.11		.22±.02	.58±.06	1.38	1.64
	12 Oct	LWR 16970	3.6	Low	7.27	1.08±.01				
	12 Oct	SWP 21276	11.1	Low	7.29		.17±.01	.43±.17	0.77	0.65
1985	07 Mar	LWP 5464	90	Hi	7.41	1.07±.11				
	07 Mar	SWP 25379	35	Low	7.49		.21±.01	.33±.04	1.05	1.05
	08 Mar	SWP 25390	30	Low	7.46		.20±.02	.29±.05	1.11	1.22
	08 Mar	LWP 5470	90	Hi	7.44	1.10±.13				
	07 Jul	LWP 6363	1.5	Low	6.89					
	07 Jul	LWP 6364	1	Low	6.89	2.63±.17				
	07 Jul	SWP 26369	4	Low	6.79					
	07 Jul	SWP 26370	778	Hi	6.79					
	08 Jul	SWP 26372	12	Low	6.74		.27±.02	.43±.17	2.39:	1.65
	08 Jul	LWP 6365	80	Hi	6.76	2.79±.26				
1986	6 Aug	SWP 28853	30	Low	7.15		.25±.02	.40±.05	0.78	0.84
1990	07 Sep	LWP 18717	85	Hi	6.90	2.35±.26				
1991	18 Sep	LWP 21268	80	Hi	6.83	2.50±.28				
	18 Sep	LWP 21267	2	Low	6.85					
	18 Sep	SWP 42497	10	Low	6.83		.27±.03	.36±.19	0.85	1.55
1992	16 Mar	LWP 22612	90	Hi	6.98	2.18±.23				
	16 Mar	SWP 44183	13	Low	7.02		.27±.03	.37±.12	0.88	0.94
	18 Mar	LWP 22632	80	Hi	6.94	2.18±.23				
	10 Sep	SWP 45591	10	Low	6.99					
	10 Sep	SWP 45592	29	Low	7.03		.274±.03	.44±.09	1.30	1.10
	10 Sep	LWP 23894	2	Low	6.96					
	10 Sep	LWP 23895	80	Hi	6.97	1.87±.19				
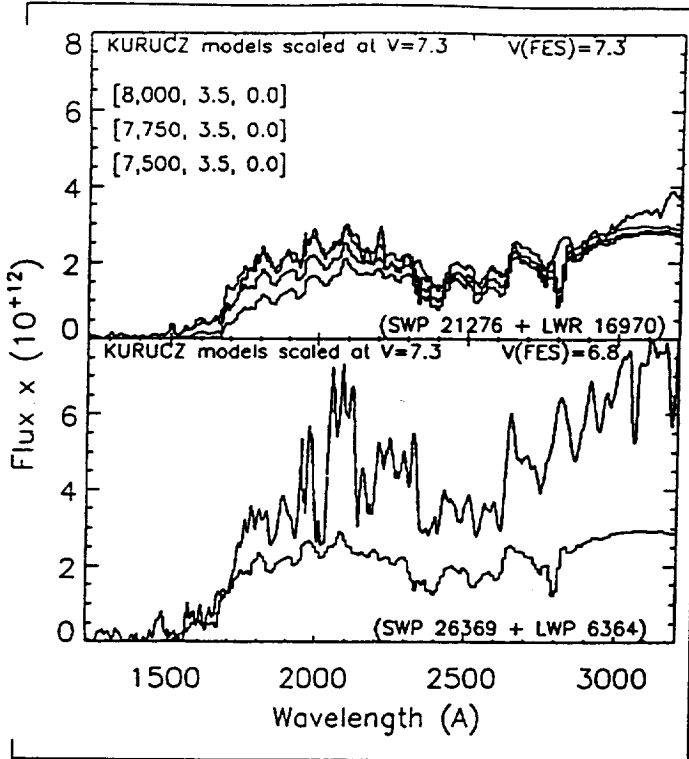
Fig. 2. Extinction-corrected UV spectral energy distributions (bold lines) for UV-faint (upper panel) and UV-bright (lower panel) states compared with Kurucz (1991) model atmospheres normalized to the V(FES) of the IUE data. Only the Kurucz model with T_{eff}=8,000, log g=3.5 and log z=0 is displayed in the lower panel. These data provide convincing evidence for excess continuum radiation compared to the inferred optical spectral type of A7 III even in the UV-faint state, and a systematic shift to earlier inferred UV spectral types with wavelength.
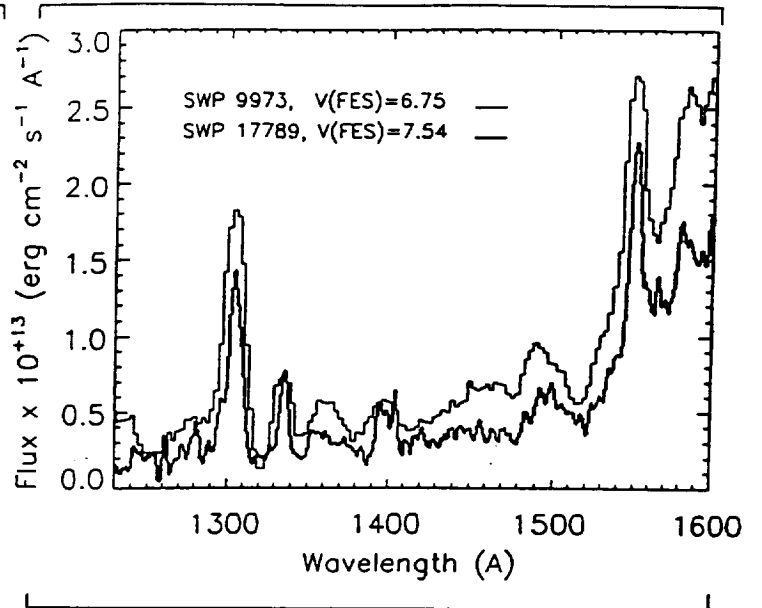

Fig. 3. Observed far-UV spectral energy distribution for representative UV-bright (SWP 9973, 31 August 1980) and UV-faint (SWP 17789, 27 August 1982) states. Both images present flux saturation for λ > 1600 Å. The IUE data demonstrate: a) the presence of a UV excess down to Lyα, b) significant continuum variability which can be followed down to 1420 Å, and c) significant changes in the net emission fluxes and velocity width of the emission of O I 1302 Å and C IV 1549 Å which are correlated with the flux variability observed at longer wavelengths.

produced in the bipolar outflows. The suggestion that this star is seen almost edge-on comes from its observed high rotational velocity, $v \sin i$=180±20 km s^{-1} (Tjin A Djie et al. 1989, ~ 66% of its break up velocity), its large infrared excesses (E(V-L)=3.2 mag) which in turn should produce high UV extinction (1.2≤ A_{2800} ≤ 2.2 mag for R_v=5.8, according to Pérez et al. 1992a), however, the Mg II, C IV, Si IV emission lines for example, appear strong and relatively unaffected by changes in extinction indicating that the emission volume generating these infrared excesses are not isotropically distributed and they are likely to be confined to a disk.

All of the HR 5999 Mg II profiles obtained through 1985 have Beals (1950) type III P Cygni profiles, despite being obtained at epochs of both high UV continuum flux (the 1979 data), and low continuum flux (all intervening spectra). When IUE observations resumed in September 1990, the character of the Mg II profile had changed drastically to Beals type III inverse P Cygni profiles closely resembling the Hα profiles of Baade and Stahl (1989) (Figure 4). Subsequent spectra obtained between 1991 and March 1992, also exhibit inverse P Cygni profiles, although not as extreme as the 1990 September observation.

When the data are normalized by division by the local continuum near 2780 Å, several features of the dataset emerge. First, the emission is more prominent relative to the contin-

uum in spectra obtained during the low UV continuum state. Spectra obtained during this epoch exhibit a broad emission base extending to +300–350 km s^{-1} which shows no changes in the far wing, as measured from the Mg II 2802 Å red emission line component. Variability in the onset of emission in the violet component of both members of the doublet is correlated with variable absorption in the Mg II (3) 2790, 2797 Å lines. Variability in the inner ±100 km s^{-1} of the profile is correlated with changes in the column density and distribution in radial velocity of the self-reversed absorption and mirror the variability in the Mg II (3) lines. Obscuration of the emission profile by intervening material producing the absorption features is therefore likely to account for the variability of the net emission flux for Mg II in both the high and low continuum states, although our data suggest that the net emission is systematically higher in the high continuum state.

Interpretation of the absorption self-reversal in Mg II hinges on knowledge of the stellar radial velocity. As noted by Tjin A Djie et al. (1989), the complexity and variability of the optical spectrum makes such measurements not only challenging, but also highly uncertain. The absence of the expected, rotationally broadened profiles consistent with the spectral type inferred near Hα throughout the UV and extending into the optical spectrum at Ca II (Lagrange-Henri et al. 1990, Tjin A Djie et al. 1989), further complicates estimates of the radial velocity. To date, the most careful determination is that of Tjin A Djie et al. (1989) which included 18 stellar lines covering the wavelength range from 3711.889 to 4508.162 Å. Their measurements of -1.6 ± 1.5 km s^{-1} and -3.2 ± 1.1 km s^{-1} (assuming that the radial velocity variability is due to circular orbital mo-

tion), at least have the merit of being in agreement with the radial velocity of the nearby, associated A star, HR 6000. If correct, such a stellar velocity would imply that the strongest optical and UV circumstellar absorption centroids have a small (20–40 km s^{-1}) blueshift.

Inspection of unsaturated, but moderately strong UV absorption lines such as Fe II 2783.695 Å shows that the absorption, even in the UV-faint spectra, has a FWHM significantly larger than the IUE high dispersion resolution. Moreover, the profiles, rather than having an approximately Gaussian shape, are frequently flat absorption troughs, or have more complex profiles which are not adequately resolved by IUE. These profiles are similar to line profiles seen in the recently identified Herbig Be star, HD 45677 (Grady et al. 1993), in which optical and UV spectropolarimetry (Schulte-Ladbeck et al. 1992) has demonstrated that the circumstellar disk is oriented strictly edge-on to our line of sight. The profiles also are similar to those seen toward FUOR-type objects (Welty et al. 1992a), which are believed to have active accretion disks and strong bipolar disk winds (Calvet et al. 1993). If such a model is applicable to HR 5999, the comparatively low velocity of the Mg II and optical absorption self-reversals compared to other Herbig Ae stars such as AB Aur (300–500 km s^{-1}, Praderie et al. 1986, Catala et al. 1987), suggests that our line of sight to HR 5999 must pass close to the disk equatorial plane and that the bulk of the low velocity absorption is produced by the gas in Keplerian orbit around the central source.

The wind model for AB Aur presented by Catala et al. (1987), in which the blueshifted Mg II absorption is interpreted as arising from a non-spherically symmetric emission volume, in the case of HR 5999 cannot explain any of the spectral variability such as the redshifted enhanced column density of the single ionized iron-peak species (Mg II, Mn II, Fe II), the continuum flux variability, and the reverse Hα and Mg II emissions recently detected. Furthermore, the blue absorption edges (wind terminal velocities in Catala's scheme) for nearly all species are nearly identical in HR 5999 indicating constant velocities for both the UV-faint and -bright states.

5.2. Mg II absorption

A distinctive feature of the HR 5999 Mg II profiles, compared to other Herbig Ae stars is the presence of self-reversed absorption superimposed on the emission profile and affecting the inner ±120 km s^{-1} or more of the profile. From -50 to 0 km s^{-1} the absorption feature is saturated in all spectra obtained to date. Assessment of the amount of absorption outside of this feature is less certain, due to the unknown emission profile. We have estimated the velocities of the maximum, positive extent of the absorption (V_{max}), the maximum negative extent of the absorption (V_{edge}), and approximate location of the centroid of the absorption in Table 2. Spectra with absorption occurring at the highest, positive velocities tend occur during UV-bright states, while the spectra with lower velocities, or evidence for excess absorption at negative velocities are preferentially observed during the UV-faint states. A tight correlation with continuum flux is not observed, and this is to be expected since the absorption data sample the circumstellar envelope in the pencil toward the star, whereas the emission profile and continuum sample the full envelope. The spectra obtained during lower continuum states exhibit at most modest evidence for accreting gas, or provide some indication of enhanced absorption

at negative velocities, e.g., outflowing gas. The most striking example of this phenomenon is provided by LWR 16769.

5.3. Veiling of the stellar photosphere near Mg II

The UV continuum data suggest that photospheric absorption from a star with the properties inferred by Tjin A Djie et al. (1989) should not be visible due to veiling by the UV excess. We have compared the Mg II profiles for HR 5999 with A5-7 V-III stars with $v \sin i \geq 100$ km s^{-1} from the IUE archives, and find no evidence for the strong Mg II absorption expected from a mid-A star photosphere. We note that at A5, absorption from Mg II (3) is largely blended with the absorption from the Mg II (1) lines. For A7 stars, the profiles essentially merge. Thus, detection of Mg II (3) absorption, which is distinctly present in all of our LW high dispersion spectra, and an absence of absorption wings from the photospheric profile on the long-wavelength side of the profile suggests that the stellar photosphere is veiled by continuum emission from the circumstellar envelope. This is consistent with the lack of detection of photospheric features in the optical at Fe II (42) (Graham 1992: private communication), or at Na I (Thé and de Winter 1992: private communication). Nevertheless, several narrow absorption emissions superimposed on the continuum can be seen, primarily in the UV-bright state (see Figure 2), which probably arise in the thick extended envelope which mimics a slowly rotating photosphere.

5.4. Singly ionized iron-peak species

The UV spectrum of HR 5999 is rich in absorption features to the ground configurations and excited levels of singly-ionized iron-peak elements (Blondel et al. 1989), and provides an opportunity to test our suggestion that the variability in the Mg II resonance profiles is due to variable column densities of accreting gas.

As noted by Blondel et al. (1989), strong absorption is present in the profiles of all of the lines of Fe II UV(1), (62), (63), (64), and (78). The profiles from the UV(1) transitions are saturated over the velocity range -50 to 0 km s^{-1}. Longward of this saturated absorption the IUE spectra obtained prior to 1990 show absorption extending to approx. 300 km s^{-1}. From 1990 onward increased absorption from 0-300 km s^{-1}, and especially pronounced from 0-200 km s^{-1} is visible in all of the Fe II UV(1) lines (see Figure 5). The two additional absorptions seen for Fe II 2944.40 and 2739.55 Å deprived us of detecting the full extend of the high velocity winds of the accreting gas, which can be clearly detected in the lower inset for Fe II 2599.40 Å. The differences in continuum flux levels in both estates, for all three lines, are within the repeatability errors and instrumental uncertainties of IUE.

Enhanced absorption can be followed to 300 km s^{-1} in the higher oscillator strength transitions of UV(62), (63), and (64) to the a^{4}D metastable (χ=1.05 eV) level, and enhanced absorption can be followed to 200 km s^{-1} in the transitions of UV(78) to the a^{4}P level (χ=1.67 eV). Inspection of absorption from lower oscillator strength Fe II transitions to excited levels, which are not saturated in any of the observations of HR 5999 to date, and which are free of significant line blending, such as Fe II 2783.61 Å (tabulated in Table 2), reveals that all portions of the circumstellar absorption profile are variable.

Table 2. Mg II 2802.795 Å and Fe II 2783.61 Å line profile measurements for the 13 high dispersion spectra. The radial velocities are tabulated as heliocentric velocities without correction for the stellar radial velocity or the +10 km s^{-1} systematic error in the IUE calibration. The uncertainty in the Mg II V/R ratio is estimated to be 0.1.

| Image | Mg II | | | Fe II | | | | |
	V/R	V_{max}	V_{edge}	$V_{Centroid}$	W_λ	V_{max}	λ_c	σ (Å)
LWR 3980	0.91	50±30	-95.3	-45.2	499	85	2783.33	0.55
LWR 4067	0.94	125±25	-105.5	-15.5	511	85	2783.85	0.56
LWR 14016	0.83	50±20	-55.4	+14.2	385	50:	2783.82	0.52
LWR 14026	0.86	20±20	-119.9	-38	309	50	2783.56	0.36
LWR 16769	0.92	0±20	-115.0	-45	567	30	2783.16	0.60
LWP 5464	0.82	20±20	-95.3	-33	333	40	2783.57	0.36
LWP 5470	0.75	20±20	-100.4	-26	452	40	2783.57	0.59
LWP 6365	0.73	100±20	-102.5	-31	508	70	2783.42	0.59
LWP 18717	1.34	>250	-97.4	-31	1102	250	2784.79	1.12
LWP 21268	1.21	175±25	-97.4	-18.6	638	150	2783.87	0.61
LWP 22612	1.16	100±20	-85.1	-15.5	535	200	2784.19	0.74
LWP 22632	1.22	100±20	-75.9	-15.5	622	100	2783.69	0.77
LWP 23895	1.00	100±20	-160.0	-45	412	70	2783.50	0.45
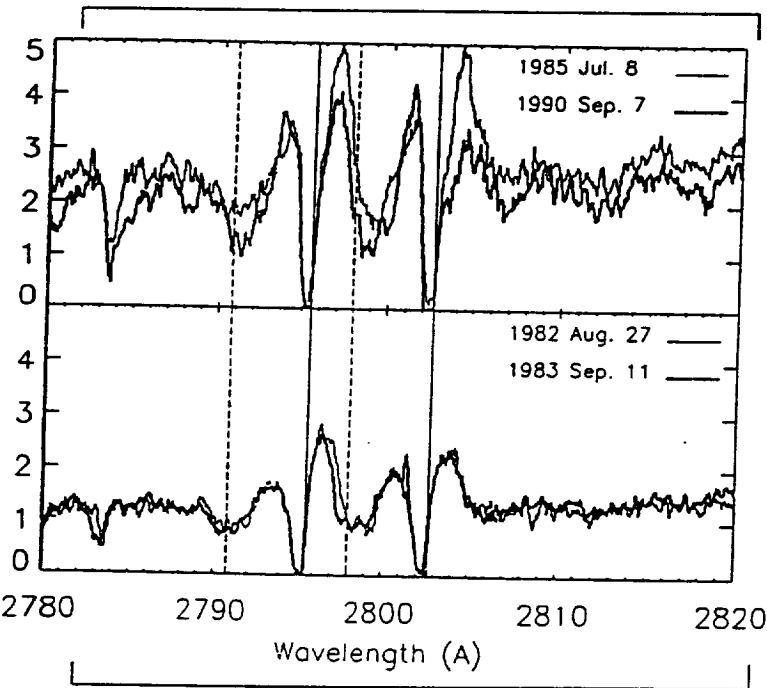
Fig. 4. Representative 2800 Å Mg II profiles for HR 5999. The upper panel shows two spectra obtained during the UV-bright state (LWP 6365, faint line; LWP 18717, bold line). Two spectra obtained during the UV-faint state are shown in the bottom panel (LWR 14026, faint line, and LWR 16769, bold line). The vertical solid lines correspond to the rest wavelengths of Mg II (UV1) and the dashed lines to Mg II (UV3).

In none of the spectra do we observe the signature of absorption from a rapidly rotating photosphere upon which the circumstellar absorption is superimposed (e.g., β Pictoris Fe II profiles presented in Boggess et al. 1991). The most dramatic

changes in the profiles, which are reflected in the equivalent width, centroid wavelength, and profile width (σ)data (Table 2) have tended to occur in spectra with enhanced high, positive velocity absorption. The exception is LWR 16769, which provides the most striking example to date of shortward-shifted absorption. The spectra with excess absorption at high, positive velocities were obtained during high continuum states for HR 5999.

Similar absorption profiles are seen in all 3 lines of Mn II UV(1) and the higher oscillator strength transitions of UV(5) (a^{5}S level, χ=1.17 eV). The Mn II UV(5) lines, which are unsaturated at the resolution of the IUE show enhanced low velocity (-10 km s^{-1}) absorption on 1990 Sept compared to LWP 6365, as well as components at 70 and 150 km s^{-1} (see Figure 6). A similar velocity structure is present in the higher oscillator strength transitions of Cr II UV(5), (6), and (8) (a^{6}D level, χ=1.51 eV). Earlier Ca II data show saturated absorption over the velocity range of the "shell" feature, with enhanced absorption extending to at least 150 km s^{-1} (see Tjin a Djie et al. 1989; and the higher-signal-to-noise ratio spectrum in Lagrange-Henri et al. 1990).

5.5. Comparison with β Pictoris

The singly ionized metal absorption profiles seen since 1990, with large column densities at low velocities and smaller column densities at progressively higher, positive velocities, are strongly reminiscent of the accreting gas profiles seen toward the proto-planetary system candidate β Pictoris (e.g., 51 Oph, Grady and Silvis 1993) Both systems have circumstellar absorption profiles characterized by large column densities near the stellar radial velocity, with decreasing absorption extending to high positive velocities in at least some spectra. Both systems exhibit high-density, high velocity gas of variable column density, absorption components in some spectra which are particularly prominent in the low velocity portion of the flow,
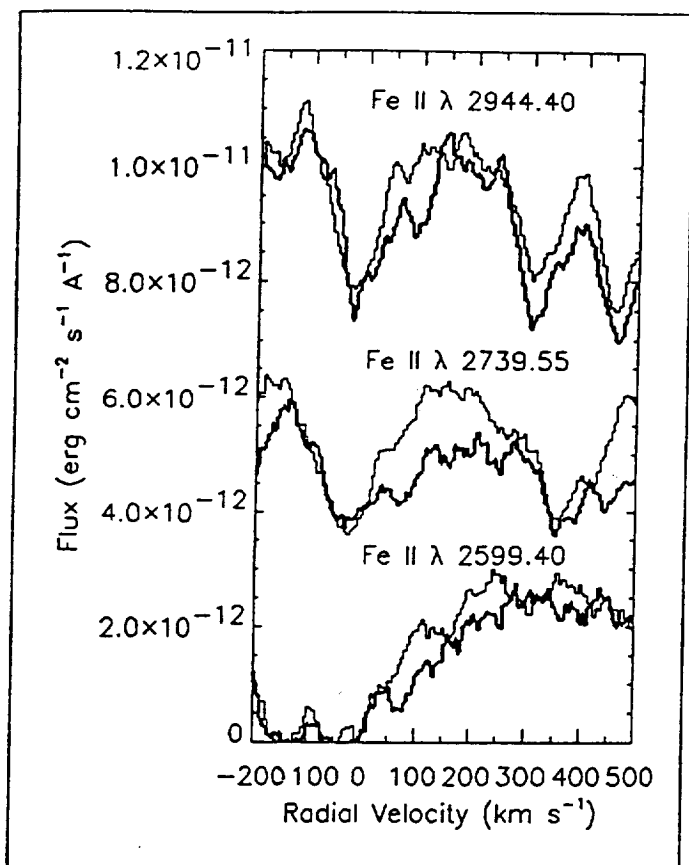
Fig. 5. Circumstellar Fe II absorption from 1985 July 8 (LWP 6365) and 1990 September (LWP 18717). The lines from top to bottom, 2944.4 Å (UV78), 2739.55 Å (UV 63) 2599.40 Å (UV1), demonstrate both the variability of the line-of-sight mass accretion rate during the UV-bright state and provide evidence for accreting gas with velocities as large as +300 km s^{-1}.

and a trend for the FWHM of the components to increase with increasing radial velocity (see Boggess et al. 1991; Lagrange-Henri et al. 1992). The relative prominence of the accreting gas relative to the material closer to the inferred systemic velocity increases with increasing excitation potential, as does the suggestion of discrete absorption components, which are particularly prominent in the 1985 July 8 and 1990 September data (Figures 4 and 5). Similarly, the outflowing material observed in LWR 16769 also becomes more prominent with increasing excitation potential. Similar behavior is observed in the accreting and outflowing gas toward β Pictoris (Bruhweiler et al. 1991, 1992; Boggess et al. 1991).

In the case of β Pictoris, higher signal-to-noise and resolution HST GHRS data have demonstrated that the excitation temperature of the accreting gas exceeds the stellar T_{eff}, and that the components have excitation temperatures above the temperature of the accreting gas at nearby velocities (Bruhweiler et al. 1992). The IUE data for HR 5999 suggest that the accreting gas in this, much younger system ($\tau \approx 5 \times 10^5$ year, $M_{acc} \approx 6.8 \times 10^{-7}$ M$\odot$ yr^{-1} Blondel et al. 1992) with a significantly higher mass accretion rate, exhibits the same phenomena. The variability of the C IV net emission fluxes, compared with O I, may indicate the presence of C IV in absorption in the line-of-sight, since the UV-bright spectra with

low C IV fluxes correspond to epochs with enhanced Mg II and Fe II absorption. If this assertion is supported by higher resolution UV spectra, such as can be provided by the HST, it will provide confirmation of the presence of collisionally ionized gas in the HR 5999 system. Detection of transient, outflowing material which is high density, and potentially collisionally ionized is a further point of similarity which must be accounted for in any model for accretion phenomena onto young, intermediate mass stars.

6. Discussion

6.1. Constraints on our viewing geometry

The double-peaked Hα and Mg II emission profiles characteristic of HR 5999 strongly suggest that we viewed the HR 5999 system close to the systemic plane, if the emission originates in a rotating circumstellar envelope (Pérez et al. 1992b). Detection of high-velocity, accreting gas in several spectra, most notably the 1990 September observation, confirms this suggestion, and further suggests that we view the HR 5999 system through a substantial portion of the circumstellar disk, if this proto-planetary system has a flattened geometry similar to that observed around β Pictoris, and inferred for HAEBE stars with IR excesses consistent with the presence of a viscously-heated disk (Hillenbrand et al. 1992), similar to those inferred for lower mass PMS stars (Strom, Edwards, and Strom 1989). Together, these data imply that the orientations of the HR 5999 and β Pictoris systems to our line of sight are similar. Comparison of the two systems may, therefore, provide particularly valuable insight into the nature and timescale of the final stages of accretion onto the proto-star and the onset of clearing of the inner portions of the debris disks in massive PMS stars.

6.2. The accretion disk and boundary layer

The presence of accretion disks around PMS stars has been inferred from the nature of the IR excess. Optically-thick disks with large IR excesses have been interpreted as indicating the presence of a debris disk which not only reprocesses the stellar radiation, but also is viscously heated. In a recent survey of HAEBE stars, Hillenbrand et al. (1992) fit such a disk model to HR 5999, and also infer the presence of a small (6 stellar radii) inner gap in the debris disk from the comparative weakness of the IR excess at 1-2 μm, assuming no excess emission at shorter wavelengths.

The presence of the hotter portions of accretion disks and boundary layers around lower mass T Tauri stars and FUORs was recognized by the presence of both excess flux at shorter wavelengths, than was expected for the inferred optical spectral type, and a trend of the inferred spectral type to shift to earlier classes with decreasing wavelength of observation (Hartmann and Kenyon 1985, 1987; Hartmann et al. 1989; Bertout, Basri, Bouvier 1988; Basri and Bertout 1989). Our UV data demonstrate both phenomena, and suggest a link with the optical photometric variability which has been interpreted as evidence for accretion instabilities (Pérez et al. 1992a). The accretion interpretation is further strengthened by the detection of enhanced line-of-sight accretion during epochs of high UV continuum luminosity. This phenomenon has not previously been observed in a HAEBE star. This association may also indicate an origin for the high velocity accreting gas as part of disk
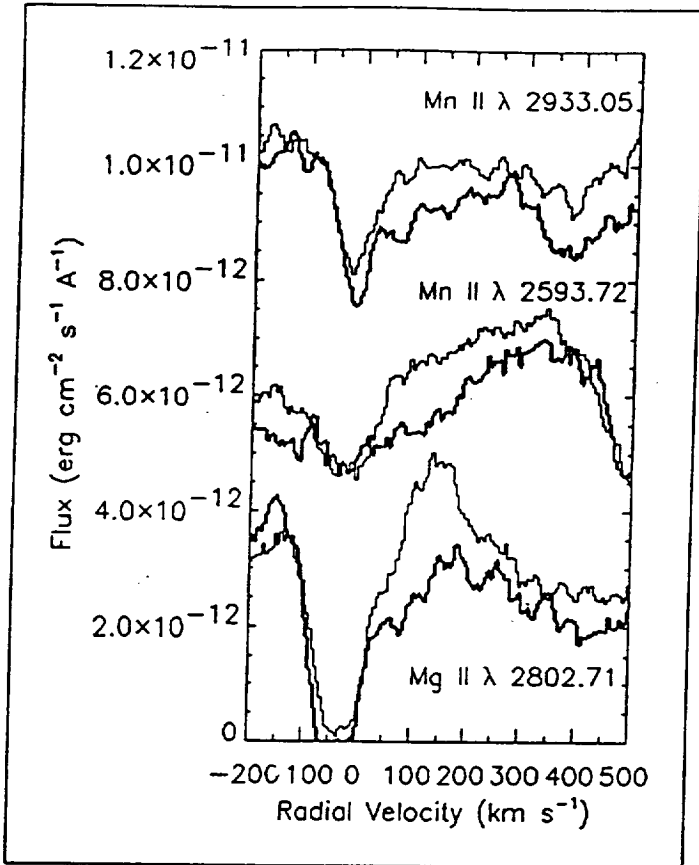
Fig. 6. Circumstellar Mn II and Mg II (h line) absorption profiles. The same spectra are shown as in Figure 4. Top: Mn II 2933.05 (UV5), middle: Mn II 2593.72 Å (UV1) and bottom: Mg II 2802.71 Å (UV1).

instabilities rather than being the signature of sporadic bombardment of the star by cometary mass bodies, as suggested for β Pictoris (Lagrange-Henri et al. 1988). Together with the detection of an apparent shift in spectral type in HD 163296 (Blondel et al. 1992), these data provide the first direct evidence for on-going accretion and the visibility of the accretion disk and boundary layer in the UV spectra of intermediate mass PMS stars. Our data, which demonstrate not only the variability of the UV excess, but also dramatic changes in the line-of-sight column density in the accretion flow, suggest that the accreting gas is clumpy. Similar conclusions based on optical data, have been reached for the R CrA and lower mass systems by Graham (1992) and for BF Orionis by Welty et al. (1992b).

6.3. How real is the cavity inferred from the IR data?

The UV continuum data for HR 5999 suggest the presence of a spatially extended, optically thick region which is producing the bulk of the UV light. In combination with the large, observed column densities of accreting gas in the line of sight, the continuum data strongly suggest that the cavity inferred from models of the IR photometry does not represent detection of a void around the star, but rather the destruction of the circumstellar grains due to viscous heating in the accretion disk and

boundary layer. Our data suggest that much of the luminosity variability of this object is not merely due to intermittent obscuration of the star by circumstellar dust clouds, as suggested by one of us (Thé 1992), but due to clumpy accretion. The presence of clumpy accretion has implications for estimates of the stellar properties based on locating the star in the HR diagram. For example, if the luminosity variations are due to obscuration, the stellar luminosity can best be estimated at maximum light. However, if the luminosity variability is due to fluctuations in the mass accretion rate, the stellar luminosity can be more accurately estimated at minimum UV light, although our data suggest substantial veiling of the star at all epochs to date.

6.4. Chromospheres versus accretion models

Previous models of the circumstellar environment of HR 5999 have interpreted the data in terms of a rotating and expanding axisymmetric envelope (c.f., Praderie et al. 1991). This interpretation was largely driven by the presence of the absorption feature seen in Mg II and Hα being interpreted as blue-shifted with respect to the unknown systemic velocity. In this model, emission in Mg II, O I, C IV and other lines originated in a "chromosphere-like" or "super-ionization" region (T$\sim$ 8 x 10^5 K) of uncertain origin (c.f., Catala et al. 1984), since the photosphere for a star in this temperature range was expected to be radiative, rather than convective. Detection of signatures of the accretion disk and boundary layer, constraints on our viewing geometry, and the realization that we do not view all the way through the circumstellar envelope to the star, suggests that a substantial revision of our picture of this, and possibly other Herbig Ae stars, is needed. The UV data for HR 5999 are consistent with the presence of an optically thick inner portion of the accretion disk or boundary layer. The luminosity of this region is driven by the variable mass accretion rate. The presence of double-peaked Hα and Mg II emission suggests that some of the emission lines originate, at least partially, in the disk, which in addition to a radial velocity component, is rotating. The Mg II emission profiles, with comparatively invariant high velocity wings, and low velocity emission which is dramatically variable suggests, together with the Lyα data discussed in Blondel et al. (1992), that some fraction of the emission may originate in a collimated bipolar flow perpendicular to the disk plane. UV spectropolarimetry of the emission lines may be helpful in distinguishing between the disk and bipolar flow contributions to the emission. Higher resolution and signal-to-noise UV spectroscopic observations of lines such as C IV will be critical in establishing the extent of collisional ionization and viscous heating of the accreting gas. The IUE data, by themselves, suggest however that the accretion phenomena are sufficiently energetic to account for the presence of highly ionized species without needing to invoke chromospheric phenomena for this proto-star.

Our line of sight to HR 5999 clearly transits a substantial portion of the disk dust, accounting for the high value of R_v, and is probably reasonably close to the equatorial plane of the system. During periods of higher UV luminosity, we observe generally higher velocities of accreting gas, as well as higher column densities of material in the line of sight. While the UV database is quite limited, detection of outflowing gas during an epoch of low UV luminosity, and minimal line-of-sight accreting gas, suggests that collimation of a bipolar flow, or disk

wind may be less efficient during episodes of low-rate mass accretion.

References

Ake, T.B. 1982, NASA IUE Newsletter 19, 37.

Ake, T.B. 1985, Record of the IUE Three Agency Coordination Meeting (NASA/ESA/SERC), Nov. 13-16, 1984 at GSFC, A-138.

Baade, D., Stahl, O. 1989, A&A, 209, 255.

Basri, G., Bertout, C. 1989, ApJ, 341, 340.

Beals, C. 1950, Publ. Dom. Astrophys. Obs., 9, 1.

Bertout, C., Basri, G., Bouvier, J. 1988, ApJ, 330, 350.

Bessel, M.S., Eggen, O.J. 1972, AJ, 177, 209.

Blondel, P.F.C., Tjin A Djie, H. R. E., Thé, P.S. 1989, A&A, 80, 115 (Paper IX).

Blondel, P.F.C., Talavera, A., Tjin A Djie, H.R.E 1992, A&A, (in press).

Boggess, A., Bruhweiler, F.C., Grady, C.A., Ebbets, D.C., Kondo, Y., Trafton, L.M., Brandt, J.C., Heap, S.R., 1991, ApJ 377, L49.

Bohlin, R.C. Holm, A.V. 1980, NASA IUE Newsletter, No. 10, 37.

Bruhweiler, F.C., Kondo, Y., Grady, C.A. 1991, ApJ 371, L27.

Bruhweiler, F.C., Lyu, H.-S., Boggess, A., Kondo, Y., Grady, C.A. 1992, ApJ (submitted).

Calvet, N., Hartmann, L., Kenyon, S.J. 1993, ApJ, 402, 623.

Cardelli, J.A., Clayton, G.C., Mathis, J.S. 1989, ApJ, 345, 245.

Cassatella, A., Harris, A.W. 1983, NASA IUE Newsletter 23, 21.

Cassatella, A., Ponz, D., Selvelli, P.L., Vogel, M. 1990, NASA IUE Newsletter 41, 155.

Catala, C., Kunasz, P.B., Praderie, F., 1984, A&A, 134, 402.

Catala, C., Praderie, F., Felenbok, P. 1987, A&A, 182, 11.

Clavel, J., Gilmozzi, R., Prieto, A. 1985, NASA IUE Newsletter 27, 50.

Grady, C.A., Silvis, J.M.S. 1993, ApJ, 402, L61.

Grady, C.A., Bjorkman, K.S., Shepherd, D., Schulte-Ladbeck, R.E., Pérez, M.R., de Winter, D., Thé, P.S. 1993, ApJ, submitted.

Graham, J.A. 1992, Pub. A.S. Pac. 104, 479.

Harris, A.W., Sonneborn, G. 1987, "How to Use IUE Data", in *Exploring the Universe with the IUE Satellite*, Kondo, Y. (ed.), (Dordrecht::Reidel).

Hartmann, L. Kenyon, S.J. 1985, ApJ, 299, 462

Hartmann, L. Kenyon, S.J. 1987, ApJ, 312, 343

Hartmann, L., Kenyon, S.J., Hewett, R., Edwards, S., Strom, K.M., Strom, S.E. 1989, ApJ, 338, 1001.

Hecht, J.H., Holm, A.V., Ake III, T.B., Imhoff, C.L., Oliversen, N.A., Sonneborn, G. 1984, in Future of Ultraviolet Astronomy based on Six years of IUE Research, Nasa Conference Publication, No. 2349, p. 318.

Hillenbrand, L.A., Strom, S.E., Vrba, F.J., Keene, J. 1992, ApJ 397, 613.

Kurucz, R.L. 1991, in Precision Photometry: Astrophysics of the Galaxy, Davis Philip, A.G., Upgren, A.R., Janes, K.A. (eds.) (Schenectady, N.Y.:: L. Davis Press).

Lagrange-Henri, A.M., Vidal-Madjar, A., Ferlet, R. 1988, A&A 190, 275

Lagrange-Henri, A.M., Ferlet, R., Vidal-Madjar, A., Beust, H., Gry, C., Lallement, R. 1990, A&A Suppl. Ser. 85, 1089.

Lagrange-Henri, A.M., Gosset, E., Ferlet, R., Vidal-Madjar, A. 1992, A&A, 264, 637.

Pérez, M. R., Webb, J., Thé, P. S. 1992a, A&A, 257, 209 (Paper X).

Pérez, M. R., Imhoff, C. L.. Thé, P. S. 1992b, Bull. A.A.S., 23, No.4, 1374.

Pérez, M. R., Loomis, C. 1991, Record of the IUE Three Agency Coordination Meeting (NASA/ESA/SERC), Nov. 19-21, 1991 at GSFC, F-13.

Praderie, F., Simon, T., Catala, C., Boesgaard, A. M. 1986, ApJ, 303, 311.

Praderie, F., Catala, C., Czarny, J., Thé, P. S., Tjin A Djie, H. R. E. 1991, A&A, 89, 91.

Schmidt-Kaler, Th. 1982, in Landolt- Börtein, edited by Springer- Verlag, Berlin and New York, New Series, Group VI, Vol. 2.

Schulte-Ladbeck, R.E. et al. 1992, ApJ, 401, L105.

Strom, S.E., Edwards, S., Strom, K.M. 1989, in The formation and Evolution of Planetary Systems, Weaver, H.A. and Danly, L. (eds.), (Cambridge::Cambridge University Press), pp.91-110.

Teays, T.J., Garhart, M.P. 1990, NASA IUE Newsletter 41, 94.

Thé, P.S. 1992, in Proceedings of the IAU Colloquium 137 on "Inside the Stars", eds. Werner W. Weiss and Annie Baglin, in press.

Thé, P.S., Tjin A Djie, H.R.E. 1978, A&A, 62, 439 (Paper I).

Thé, P.S., Tjin A Djie, H.R.E., Bakker, R.s, Bastiaansen, P.S., Burger, M., Cassatella, A., Fredga, K., Gahm, G.F., Liseau, R., Smyth, M.J., Viotti, R., Wamsteker, W., Zeuge, W. 1981, A&AS, 44, 451 (Paper V).

Thé, P.S., Tjin A Djie, H.R.E., Brown, A., Catala, C., Doazan, V., Linsky, J.L., Mewe, R., Praderie, F., Talavera, A., Zwaan, C. 1985, Irish AJ, 17, 79.

Tjin A Djie, H.R.E., Thé, P.S., Andersen, J., Nordstrom, B., Finkenzeller, U., Jankovics, I. 1989, A&AS, 78, 1 (Paper VIII).

Turnrose, B.E., Thompson, R.W. 1984, "IUE Image Processing Information Manual Version 1.1", CSC/TM-81/6268.

Welty, A.D., Strom, S.E., Edwards, S., Kenyon, S.J., Hartmann, L.W., 1992a, ApJ, 397, 260.

Welty, A.D., Barden, S., Huenemoerder, D.P., Ramsey, L.W. 1992b, AJ, 103, 1673.

Wu, C.C., Ake, T.B., Boggess, A., Bohlin, R.C., Imhoff, C.L., Holm, A.V., Levay, Z.G., Panel, R.J., Schiffer III, F.H., Turnrose, B.E. 1983, NASA IUE Newsletter, 22.